VETOR

# Spectral-Nodal Deterministic Methodology for Neutron Shielding Calculations using the $X, Y$ – geometry Multigroup Transport Equation in the Discrete Ordinates Formulation

## Metodologia Espectronodal Determinística para Cálculos de Blindagem de Nêutrons usando a Equação de Transporte Multigrupo Considerando Problemas Bidimensionais na Formulação das Ordenadas Discretas

Amaury Muñoz Oliva[1,†], Hermes Alves Filho[2]

[1]*Instituto de Pesquisas Energéticas e Nucleares, São Paulo, Brasil*
[2]*Instituto Politécnico, Universidade do Estado do Rio de Janeiro, Nova Friburgo, Brasil*
[†]**Corresponding author:** amaury.oliva@ipen.br

**Abstract**

In this work, we present the most recent numerical results in a nodal approach, which resulted in the development of a new numerical spectral nodal method. This method is based on the spectral analysis of the multigroup, isotropic scattering neutron transport equations in the discrete ordinates ($S_N$) formulation for fixed-source calculations in non-multiplying media (shielding problems). The numerical results refer to simulations of typical problems from the neutron shielding area, in two-dimensional Cartesian geometry and are compared with the traditional Diamond Difference fine-mesh method results, used as a reference, and the spectral Green's function - constant nodal ($SGF - CN$) method results.

**Keywords**

Neutron Transport Theory • Shielding Calculations • Spectral Nodal Method

**Resumo**

Neste trabalho, apresentamos os mais recentes resultados numéricos de uma abordagem nodal (malha grossa), que resultou no desenvolvimento de um novo método da classe dos espectro-nodais, na formulação determinística das ordenadas discretas (SN), aplicado no cálculo de transporte de nêutrons multigrupo, considerando problemas de blindagem (fonte-fixa). Estes resultados numéricos se referem às simulações de problemas típicos da área de física de reatores, em geometria bidimensional cartesiana retangular e são comparados com o tradicional método de malha fina Diamond Difference (DD), usado como referência e o método de malha grossa spectral Green's function (SGF).

**Palavras-chave**

Teoria de transporte de nêutrons • Cálculos de Blindagem • Métodos Espectronodais

## 1 Introduction

Modeling neutron transport problems is a complex task and to solve it is necessary to adopt a mathematical/computational strategy. The solution may be following the line of the probabilistic school, whose basic philosophy is to

approximately solve the exact problem, eg, Monte Carlo methods [1], or the deterministic school whose philosophy is to solve exactly an approximate problem, i.e., $S_N$ discrete ordinate methods [2].

The study of deterministic mathematical models for the neutral particle transport theory has its origins within the Boltzmann equation, first formulated for the kinetic theory of gases more than a century ago [3]. The mathematical methods used to solve these transport equations have been developed to analyze radiative transfer problems in the 1930s [4, 5]. The neutron transport field was developed almost independently of the gases theory or the radioactive theory, the main reason for the attention given to the neutron transport theory, was its belonging to the atomic energy program, highly developed in the early years of the nuclear age.

The linearized Boltzmann transport equation for neutrons, in its general form, is characterized as a first-order linear partial integro–differential equation. It depends on seven independent variables: three spatial coordinates, two angular $(\mu, \eta)$, one for the neutron energy $(E)$, and one for time $(t)$ [2, 3], to describe the average behavior of the entire neutron population which shows a high complexity for its solution.

The nodal schemes (coarse mesh), as deterministic models, constitute a class of numerical methods developed to generate precise solutions for the Boltzmann equation for neutron transport [6, 7]. These methods are algebraically and computationally more laborious than the traditional fine-mesh numerical methods, i.e., the Diamond Difference (DD) method, [2], however, they present greater precision in numerical solutions for coarser spatial grids. For this reason, these numerical methods, and their possible solution algorithms using direct or iterative schemes, have been the focus of several studies in recent years [8, 9, 10].

Solve the neutron transport problems in the $S_N$ formulation, for two-dimensional Cartesian geometry, using a fine mesh method such as $DD$, also presents a series of disadvantages from the computational point of view. Among them we can mention the difficulty to obtain solutions with good precision, demanding great refinement of the spatial domain used, resulting in a high computational cost. It would be convenient to perform a discretization of the spatial variables, using coarse mesh (nodal) methods, as a way to reduce this cost without affecting the precision of the results. Within this context, we can mention the numerical methods of spectral-nodal class [11, 8, 12, 13, 14], which had their genesis with the work of Larsen [15]. To determine the discretized equations for these nodal methods, in addition to the use of the $S_N$ equations, there are also utilize auxiliary equations in the nodes of the analyzed regions. These equations hold parameters that are determined in such a way as to preserve the local analytic general solution of the problem within each spatial node, increasing the degree of complexity in obtaining the constitutive equations of these methods.

Opposite to what is made with the traditional spectral-nodal numerical methods to solve the neutron transport equation in the $S_N$ formulation; where it is necessary to obtain the auxiliary equations, burdening the simulations from the point of view of algebraic development and probable time of execution of the computational codes; it was proposed to obtain the discrete neutron transport equations, in the formulation of Discrete Ordinates, $S_N$, starting from the calculation of arbitrary parameters for the solution of the intra-nodal $S_N$ equations, initially knowing the incident fluxes and the neutron sources inside the spatial nodes of the grid of the studied problem. With this procedure, it is possible to obtain all the outgoing angular fluxes in the boundaries of the spatial nodes, to calculate some other quantities of interest for this type of simulation, such as the scalar fluxes, absorption rates in the homogeneous regions of the spatial domain, and neutron leakage rates in the external boundaries of the analyzed domain. The procedure described above was the baseline for the development of the Spectral Deterministic Method (SDM) [9, 16, 17, 18] and the Response Matrix (RM) method [10].

In this work we present the most recent advances in the development of the Spectral Deterministic Method, SDM, for neutron shielding problems, considering the multigroup neutron transport equation, $X, Y$ geometry, in the formulation of discrete ordinates $(S_N)$, where the transverse leakage terms were treated as constants.

This paper is organized as follows: The Section 2. presents the Mathematical Preliminaries with the spectral analysis of multigroup transport equations in discrete ordinates formulation in $X, Y$ geometry. Section 3., introduce and describe the iterative methodology of the multigroup Spectral Deterministic Method – Constant Nodal (SDM – CN) in $X, Y$ geometry. Section 4 presents the comparison of the numerical results of the $SDM - CN$ with the results of the $DD$, $SGF - CN$, and other methods to verify its accuracy and consistency. Finally, Section 5 exposes a brief discussion of the results and suggestions for future work within this line of development.

## 2 Mathematical Development

Considering the $S_N$ stationary equations in a rectangular domain D of width X and height Y, with linearly anisotropic scattering and interior fixed – source ($Q_g$):

$$\mu_m \frac{\partial}{\partial x}\psi_{m,g}(x,y) + \eta_m \frac{\partial}{\partial y}\psi_{m,g}(x,y) + \sigma_{T_g}(x,y)\psi_{m,g}(x,y) = \frac{1}{4}\sum_{g'=1}^{G}\{\sigma^{(0)}_{s_{g'\to g}}(x,y)\sum_{n=1}^{M}\psi_{n,g'}(x,y)\omega_n + 3\sigma^{(1)}_{s_{g'\to g}}(x,y)\mu_m\sum_{n=1}^{M}\mu_n\psi_{n,g'}(x,y)\omega_n + 3\sigma^{(1)}_{s_{g'\to g}}(x,y)\eta_m\sum_{n=1}^{M}\eta_n\psi_{n,g'}(x,y)\omega_n\} + Q_g(x,y), \quad (1)$$

where $\psi_{m,g}(x,y) \equiv \psi_g(x,y,\mu_m,\eta_m)$,

with prescribed boundary conditions represented in the form

$$\begin{aligned}
\psi_{m,g}(0,y) &= p_{m,g}(y), \quad \mu_m > 0,\\
\psi_{m,g}(X,y) &= q_{m,g}(y), \quad \mu_m < 0,\\
\psi_{m,g}(x,0) &= u_{m,g}(x), \quad \eta_m > 0,\\
\psi_{m,g}(x,Y) &= v_{m,g}(x), \quad \eta_m < 0.
\end{aligned} \quad (2)$$

for $g = 1:G$, $m = 1:M$, M represents the total number of discrete directions, which for the $x$, $y$ geometry case, is calculated by the expression

$$M = \frac{N(N+2)}{2}, \quad (3)$$

$N$ is the approximation order $S_N$. The angular quadrature, used for this work is the $LQ_N$ quadrature (*Level Symmetric Quadrature*) [2], where the $\omega_m$ are the weights of the angular quadrature associated to the discrete directions represented by the pair $(\mu_m, \eta_m)$.

Considering an arbitrary $\Omega_x \times \Omega_y$ spatial grid on the domain D, as shown in Fig.1, where each spatial cell $\Gamma_j$ have width $h_{x_i}$ and height $h_{y_j}$, constant macroscopic cross sections $\sigma^{(0)ij}_{s_{g'\to g}}$, $\sigma^{(1)ij}_{s_{g'\to g}}$, $\sigma^{ij}_{T_g}$ and constant interior source $Q^{ij}_g$. For each region analyzed in $D$,

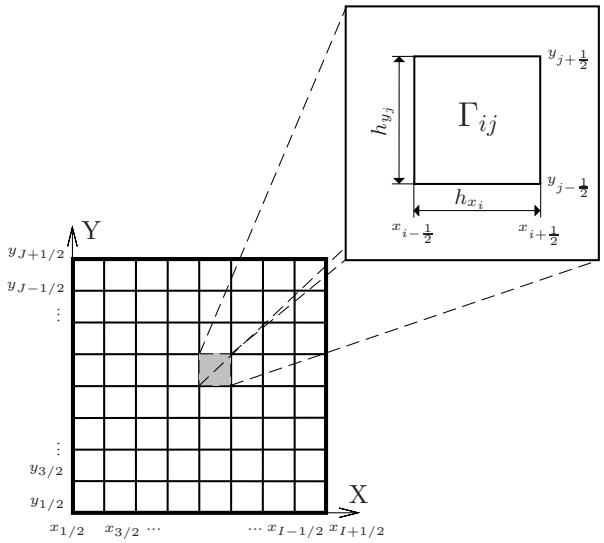



Figure 1: Discretization of the two-dimensional domain $D$ in $I \times J$ spatial cells $\Gamma_{ij}$ of width $h_{x_i}$ and height $h_{y_j}$

$\sigma_{T_g}(x,y)$, describe the g-th group macroscopic total cross section

$\sigma^{(0)}_{s_{g'\to g}}(x,y)$, represents the zero'th component of the macroscopic g-th differential scattering cross section from group g' to group g,

$\sigma^{(1)}_{s_{g'\to g}}(x,y)$, first – order component of the macroscopic g-th differential scattering cross section from group g' to group g,
$Q_g(x,y)$, isotropic neutron source in energy group g.
It is assumed that these quantities are piecewise constant functions in $D$ [13].

In order to obtain the one–dimensional transverse – integrated $S_N$ nodal equations with linearly anisotropic scattering, the transverse–integration operators, are defined

$$\frac{1}{h_{u_s}}\int_{u_{s-\frac{1}{2}}}^{u_{s+\frac{1}{2}}}(\cdot)du\ , \tag{4}$$

where $u = x$ (or $y$) and $s = i$ (or $j$).

At first we choose to integrate the Eq. (1) in the $y$ direction, where $u = y$ and $s = j$, to obtain the transverse–integrated $S_N$ nodal equation for the $x$ direction

$$\mu_m\frac{d}{dx}\widetilde{\psi}^j_{m,g}(x)+\frac{\eta_m}{h_{y_j}}\left(\psi^{j+\frac{1}{2}}_{m,g}(x)-\psi^{j-\frac{1}{2}}_{m,g}(x)\right)+\sigma^{ij}_{T_g}\widetilde{\psi}^j_{m,g}(x)=\frac{1}{4}\sum_{g'=1}^{G}\{\sigma^{(0)\,ij}_{s_{g'\to g}}\sum_{n=1}^{M}\widetilde{\psi}^j_{n,g'}(x)\omega_n$$
$$+3\sigma^{(1)\,ij}_{s_{g'\to g}}\mu_m\sum_{n=1}^{M}\mu_n\widetilde{\psi}^j_{n,g'}\omega_n+3\sigma^{(1)\,ij}_{s_{g'\to g}}\eta_m\sum_{n=1}^{M}\eta_n\widetilde{\psi}^j_{n,g'}(x)\omega_n\}+Q^{ij}_g\quad ,$$
$$x\in\Gamma_{ij},\quad i=1:I,\quad j=1:J,\quad \mathrm{m}=1:\mathrm{M},\quad g=1:\mathrm{G}\ . \tag{5}$$

Similarly, is applied the operator (4) to Eq. (1) considering $u = x$ and $s = i$ and Eq. (1) is integrated over $x$ to obtain the one-dimensional transverse-integrated $S_N$ nodal equation for the $y$ direction

$$\frac{\mu_m}{h_{x_i}}\left(\psi^{i+\frac{1}{2}}_{m,g}(y)-\psi^{i-\frac{1}{2}}_{m,g}(y)\right)+\eta_m\frac{d}{dy}\widehat{\psi}^i_{m,g}(y)+\sigma^{ij}_{T_g}\widehat{\psi}^i_{m,g}(y)=\frac{1}{4}\sum_{g'=1}^{G}\{\sigma^{(0)\,ij}_{s_{g'\to g}}\sum_{n=1}^{M}\widehat{\psi}^i_{n,g'}(y)\omega_n$$
$$+3\sigma^{(1)\,ij}_{s1_{g'\to g}}\mu_m\sum_{n=1}^{M}\mu_n\widehat{\psi}^i_{n,g'}(y)\omega_n+3\sigma^{(1)\,ij}_{s_{g'\to g}}\eta_m\sum_{n=1}^{M}\eta_n\widehat{\psi}^i_{n,g'}(y)\omega_n\}+Q^{ij}_g\quad ,$$
$$y\in\Gamma_{ij},\quad i=1:I,\quad j=1:J,\quad \mathrm{m}=1:\mathrm{M},\quad g=1:\mathrm{G}\ , \tag{6}$$

where the group mean angular fluxes in each coordinate direction inside the $\Gamma_{i\,j}$ node are defined by

$$\widetilde{\psi}^j_{m,g}(x)=\frac{1}{h_{y_j}}\int_{y_{j-\frac{1}{2}}}^{y_{j+\frac{1}{2}}}\psi_{m,g}(x,y)\,dy \tag{7}$$

and

$$\widehat{\psi}^i_{m,g}(y)=\frac{1}{h_{x_i}}\int_{x_{i-\frac{1}{2}}}^{x_{i+\frac{1}{2}}}\psi_{m,g}(x,y)\,dx\ . \tag{8}$$

The equations (5) and (6) represent two systems of $GM$ ordinary differential equations in coordinate directions $x$ and $y$, respectively. Each system has $2GM$ unknowns, $GM$ unknowns represented by $\widetilde{\psi}^j_{m,g}(x)$ (or $\widehat{\psi}^i_{m,g}(y)$) and $GM$ unknowns represented by the transverse leakage terms. We assume that these transverse leakage terms are constant along the edges in each $\Gamma_{i\,j}$ nodes, constituting the only approximation performed at calculations in this work [14] [19]. Then, these transverse leakage terms approximation are presented as

$$\frac{\eta_m}{h_{y_j}}\left(\psi^{j+\frac{1}{2}}_{m,g}(x)-\psi^{j-\frac{1}{2}}_{m,g}(x)\right) \tag{9}$$

and

$$\frac{\mu_m}{h_{x_i}}\left(\psi^{i+\frac{1}{2}}_{m,g}(y)-\psi^{i-\frac{1}{2}}_{m,g}(y)\right)\ . \tag{10}$$

Considering this, it is assumed that these constants correspond to the mean values of the angular fluxes along the sides of the analyzed node, therefore

$$\psi_{m,g}^{j\pm\frac{1}{2}}(x) \approx \widehat{\psi}_{m,g}^{i,j\pm\frac{1}{2}} \tag{11}$$

and

$$\psi_{m,g}^{i\pm\frac{1}{2}}(y) \approx \widetilde{\psi}_{m,g}^{i\pm\frac{1}{2},j} \quad . \tag{12}$$

After assuming these approximations, the transverse leakage terms can be defined as

$$\frac{\eta_m}{h_{y_j}}\left(\widehat{\psi}_{m,g}^{i,j+\frac{1}{2}} - \widehat{\psi}_{m,g}^{i,j-\frac{1}{2}}\right) = \widehat{L}_{m,g}^{i,j}\,, \tag{13}$$

and

$$\frac{\mu_m}{h_{x_i}}\left(\widetilde{\psi}_{m,g}^{i+\frac{1}{2},j} - \widetilde{\psi}_{m,g}^{i-\frac{1}{2},j}\right) = \widetilde{L}_{m,g}^{i,j}\,. \tag{14}$$

Consider constant approximations for the transverse leakage terms, the objective is to ensure the uniqueness for the solution of the transversally integrated $S_N$ equations within each spatial discretization node, $\Gamma_{ij}$, with the boundary conditions and the continuity conditions at the interfaces of the nodes. In other words, to obtain two systems with $GM$ equations and $GM$ unknowns, coupled by the transverse leakage terms [19][20]. The constants to approximate these terms are chosen conveniently because it is desired to preserve the average fluxes on the sides of the node $\Gamma_{ij}$. Therefore, using the definitions (13) and (14) in Eqs. (5) and (6), we can rewrite the $S_N$ transversely integrated equations in the form

$$\begin{aligned}\mu_m\frac{d}{dx}\widetilde{\psi}_{m,g}^{j}(x) + \widehat{L}_{m,g}^{i,j} + \sigma_{T_g}^{ij}\widetilde{\psi}_{m,g}^{j}(x) = \frac{1}{4}\sum_{g'=1}^{G}\{\sigma_{s_{g'\to g}}^{(0)\,ij}\sum_{n=1}^{M}\widetilde{\psi}_{n,g'}^{j}(x)\omega_n \\ + 3\sigma_{s_{g'\to g}}^{(1)\,ij}\mu_m\sum_{n=1}^{M}\mu_n\widetilde{\psi}_{n,g'}^{j}\omega_n + 3\sigma_{s_{g'\to g}}^{(1)\,ij}\eta_m\sum_{n=1}^{M}\eta_n\widetilde{\psi}_{n,g'}^{j}(x)\omega_n\} + Q_g^{ij}\ ,\ , \\ x\in\Gamma_{ij},\quad i=1:I,\quad j=1:J,\quad \mathrm{m}=1:\mathrm{M},\quad g=1:\mathrm{G}\,. \end{aligned} \tag{15}$$

and

$$\begin{aligned}\widetilde{L}_{m,g}^{i,j} + \eta_m\frac{d}{dy}\widehat{\psi}_{m,i}(y) + \sigma_{T_g}^{ij}\widehat{\psi}_{m,i}(y) = \frac{1}{4}\sum_{g'=1}^{G}\{\sigma_{s_{g'\to g}}^{(0)\,ij}\sum_{n=1}^{M}\widehat{\psi}_{n,g'}^{i}(y)\omega_n \\ + 3\sigma_{s_{g'\to g}}^{(1)\,ij}\mu_m\sum_{n=1}^{M}\mu_n\widehat{\psi}_{n,g'}^{i}(y)\omega_n + 3\sigma_{s_{g'\to g}}^{(1)\,ij}\eta_m\sum_{n=1}^{M}\eta_n\widehat{\psi}_{n,g'}^{i}(y)\omega_n\} + Q_g^{ij}\ , \\ y\in\Gamma_{ij},\quad i=1:I,\quad j=1:J,\quad \mathrm{m}=1:\mathrm{M},\quad g=1:\mathrm{G}\,. \end{aligned} \tag{16}$$

The equations systems (15) and (16), considering a bi–dimensional domain, with uniform physical material parameters in each $\Gamma_{ij}$ node to be analyzed, have a general solution, in the form

$$\widetilde{\psi}_{m,g}(x) = \widetilde{\psi}_{m,g}^{h}(x) + \widetilde{\psi}_{m,g}^{p}\,,\ x\in\Gamma_{ij}\ , \tag{17}$$

for the equation system (15), and

$$\widehat{\psi}_{m,g}(y) = \widehat{\psi}_{m,g}^{h}(y) + \widehat{\psi}_{m,g}^{p}\,,\ y\in\Gamma_{ij}\ , \tag{18}$$

for the equation system (16). Here the superscript $p$ indicates the particular solution that is spatially constant in $D_{i\,j}$ and the superscript $h$ indicates the homogeneous component of the solution, which satisfies the homogeneous equation associated with Eqs. (15) and (16). In order to determine the particular solution of the system (15), the fluxes $\widetilde{\psi}_{m,g}^{j}(x)$ are substituted for $\widetilde{\psi}_{m,g}^{p}$, obtaining

$$\begin{aligned}\frac{1}{4}\sum_{g'=1}^{G}\sum_{n=1}^{M}\left(4\sigma_{T_g}^{ij}\delta_{mn}\delta_{g'g} - \left[\sigma_{s_{g'\to g}}^{(0)\,ij} + 3\sigma_{s_{g'\to g}}^{(1)\,ij}\{\mu_m\mu_n + \eta_m\eta_n\}\right]\omega_n\right)\widetilde{\psi}_{n,g'}^{p} = Q_g^{ij} - \widehat{L}_{m,g}^{i,j}\ , \\ \mathrm{m}=1:\mathrm{M},\quad g=1:\mathrm{G}\,. \end{aligned} \tag{19}$$

$$\text{where } \delta_{a,b} = \begin{cases} 1 & \text{para} \quad a = b \\ 0 & \text{para} \quad a \neq b \end{cases} \text{, represents the } \textit{Krönecker delta.}$$

Making the same analysis for the system given in Eq. (16), it is obtained

$$\frac{1}{4}\sum_{g'=1}^{G}\sum_{n=1}^{M}\left(4\sigma_{T_g}^{ij}\delta_{mn}\delta_{g'g} - \left[\sigma_{s_{g'\to g}}^{(0)\,ij} + 3\sigma_{s_{g'\to g}}^{(1)\,ij}\{\mu_m\mu_n + \eta_m\eta_n\}\right]\omega_n\right)\widehat{\psi}_{n,g'}^{p} = Q_g^{ij} - \widetilde{L}_{m,g}^{i,j} \quad ,$$

$$\mathrm{m} = 1:\mathrm{M}, \quad g = 1:\mathrm{G}\,. \quad (20)$$

The homogeneous solution of Eq. (15) has the form

$$\widetilde{\psi}_{m,g}^{hj}(x) = a_{m,g}^{x}(\nu^x)e^{\dfrac{-\left(x - x_{j-\frac{1}{2}}\right)}{\nu^x}} \quad , \quad m = 1:\mathrm{M}, \quad x \in \Gamma_{\mathrm{j}}\,, \quad (21)$$

Substituting the equation (21) into the homogeneous part of Eq. (15), considering the source $Q_g^{ij} = 0$ and $\widehat{L}_{m,g}^{i,j} = 0$, is obtained

$$\frac{1}{4\mu_m}\sum_{g'=1}^{G}\sum_{n=1}^{M}\left(4\sigma_{T_g}^{ij}\delta_{g'g}\delta_{mn} - \left[\sigma_{s_{g'\to g}}^{(0)\,ij} + 3\sigma_{s_{g'\to g}}^{(1)\,ij}\{\mu_m\mu_n + \eta_m\eta_n\}\right]\omega_n\right)a_{n,g'}^{x}(\nu^x) =$$

$$\frac{1}{\nu^x}a_{m,g}^{x}(\nu^x) \quad ,$$

$$\mathrm{m} = 1:\mathrm{M}, \quad g = 1:\mathrm{G}\,. \quad (22)$$

An analogous procedure to that done for Eq. (15), can be performed to solve the system of equations (16), considering for this case $\widetilde{L}_{m,g}^{i,j} = 0$, obtaining the system of equations

$$\frac{1}{4\eta_m}\sum_{g'=1}^{G}\sum_{n=1}^{M}\left(4\sigma_{T_g}^{ij}\delta_{g'g}\delta_{mn} - \left[\sigma_{s_{g'\to g}}^{(0)\,ij} + 3\sigma_{s_{g'\to g}}^{(1)\,ij}\{\mu_m\mu_n + \eta_m\eta_n\}\right]\omega_n\right)a_{n,g'}^{y}(\nu^y) =$$

$$\frac{1}{\nu^y}a_{m,g}^{y}(\nu^y) \quad ,$$

$$\mathrm{m} = 1:\mathrm{M}, \quad g = 1:\mathrm{G}\,. \quad (23)$$

Both equations (22) and (23), in a matrix notation, can be written in the form

$$A\mathbf{a}(\nu) = \frac{1}{\nu}\mathbf{a}(\nu),$$

where, similar to the one-dimensional case [21], A is a square real matrix, of order $GM \times GM$, and the eigenvalues $\nu_\ell$ are all symmetric and appear in pairs of opposite signs, due to the symmetry of angular quadrature used.

Therefore, the local general solution for each $S_N$ equations system within each node$\Gamma_{ij}$, (15) and (16), respectively, appear in the form

$$\widetilde{\psi}_{m,g}^{j}(x) = \sum_{\ell=1}^{GM}\alpha_\ell^x\, a_{m,g}^{x}(\nu_\ell^x)\, e^{\dfrac{-\left(x - x_{i-\frac{1}{2}}\right)}{\nu_\ell^x}} + \widetilde{\psi}_g^p \quad , \quad m = 1:\mathrm{M}, \quad g = 1:\mathrm{G}, \quad x \in \Gamma_{\mathrm{ij}} \quad (24)$$

and

$$\widehat{\psi}_{m,g}^{i}(y) = \sum_{\ell=1}^{GM}\alpha_\ell^y\, a_{m,g}^{y}(\nu_\ell^y)\, e^{\dfrac{-\left(y - y_{j-\frac{1}{2}}\right)}{\nu_\ell^y}} + \widehat{\psi}_{\mathrm{g}}^p \quad , \quad m = 1:\mathrm{M}, \quad g = 1:\mathrm{G}, \quad y \in \Gamma_{\mathrm{ij}}\,, \quad (25)$$

where the parameters $\alpha_\ell^x$ and $\alpha_\ell^y$ are arbitrary constants to be determined according to the boundary conditions of the spatial discretization node.

# 3 Iterative process of the multigroup Spectral Deterministic Method–Constant Nodal(SDM–CN)

In this section it is described the iterative process for solving the $SDM - CN$ neutron transport equation, spatially and angularly discretized in the multigroup formulation [22].

After obtaining the $\alpha_\ell^x$ and $\alpha_\ell^y$ parameters, the outgoing fluxes of the analyzed node are computed using the same equations, (24) and (25). Then, the $\alpha_\ell$ parameters and the outgoing fluxes at each spatial node's output are calculated using Eqs.(24) and (25). Reached this point, it becomes necessary to define the concept of sweeping the spatial discretization $x, y$ geometry grid, to understand the dynamics of calculating the outgoing angular fluxes in the $SDM - CN$ iterative scheme. Similarly to the iterative algorithm of the $SDM$ method for one-dimensional problems [21], the iterative algorithm for the $X, Y$ geometry case is essentially different from the transport sweeps employed by the methods $DD$ [2] and $SGF - CN$ [12].

By defining the sweeping concept for a $X, Y$ geometry spatial discretization grid using the $SDM - CN$ method, the coordinate system in Cartesian plane is initially taken as reference. The coordinate axes $(\mu_m; \eta_m)$ are oriented in the directions of $(x; y)$ respectively. Both axes range from negative to positive in the Cartesian coordinate system.

The numerical iterative process [9] is initiated by performing the spectral analysis of Eqs. (5) and (6) at the chosen node to start the sweeping process. This node $\Gamma_{i,j}$ can be located on the first or last row of the spatial discretization grid by combining it with the first or last column of the same grid. For this paper, we establish the starting node at the combination, first bottom row with first column on the left side. Once obtained the $a_{m,g}^x(\nu_\ell^x)$ and $a_{m,g}^y(\nu_\ell^y)$ eigenvectors with the corresponding eigenvalues $\nu_\ell$ together with the particular solutions $\widetilde{\psi}_{n,g}^p$ and $\widehat{\psi}_{n,g}^p$ we proceed with the calculation of the $\alpha_\ell^x$ and $\alpha_\ell^y$ parameters at the first node $\Gamma_{i,j}$ using the Eqs. (24) and (25) together with the pre-established boundary conditions on the left and lower sides of the node. For the incoming angular fluxes on the upper and right interfaces of the analyzed node, an initial estimate is made. Obtained the $\alpha_\ell^x$ and $\alpha_\ell^y$ parameters in the first node, using again the Eqs. (24) and (25), it can be determined the outgoing angular fluxes of first node in all energy groups.

Advancing to the right of the starting node, applying the continuity conditions we can use the outgoing angular fluxes in all energy groups in the right interface of this node as initial approximation for the incoming angular fluxes for the left side of the adjacent node. In the adjacent node, the incoming angular fluxes on the right and top interfaces continue as initial approximations. With the approximation of the incoming angular fluxes on the node, is possible to calculate the $\alpha_\ell$ parameters and the outgoing angular fluxes.

Going from left to right of the initial $\Gamma_{i,j}$ node at the initial line, the Eqs. (24) and (25) are used to determine the $\alpha_\ell$ parameters and the outgoing angular fluxes, $\widetilde{\psi}_{m,g}^j$ and $\widehat{\psi}_{m,g}^i$, at the interfaces of the remaining nodes. When the opposite end of the exit point is reached in the direction of $x$, in this case, it is switched to the next line in the direction of $y$ and the movement starts again from left to right on the new line. The Eqs. (24) and (25) are still being used to determine the parameters $\alpha_\ell$, and the outgoing angular fluxes $\widetilde{\psi}_{m,g}$ and $\widehat{\psi}_{m,g}$ at the $\Gamma_{i,j}$ cells interfaces.

Finishing the calculations for all nodes in the grid, it is checked whether the stopping criterion is satisfied. This criterion establishes that the relative deviation between two consecutive estimates for the scalar flux at the energy groups on the node-edge does not exceed a pre-established $\varepsilon$ positive value. If the stopping criterion is satisfied, the algorithm is terminated.

The updating of the transversal leakage terms and the particular solutions in each $\Gamma_{ij}$ nodes is always carried out using the physical-material parameters of these nodes together with the boundary conditions and/or the estimates of the incoming angular fluxes at each one of these nodes. These estimates for the angular fluxes incoming on the nodes $\Gamma_{ij}$ are constantly updated as the iterative process progresses.

# 4 Numerical Results

In this section we examine two $X, Y$ geometry model problems. The first is a heterogeneous domain developed by Barros and Larsen [13]. The results of the *SGF–CN* method are compared with the results obtained through the spectral nodal methodology *SDM–CN*.

This problem considers a 100 $cm \times 100$ $cm$ spatial domain with an isotropic unitary neutrons source, $Q_1 = 1\,(cm^{-3}s^{-1})$, at the center surrounded by a shielding material, $Q_2 = 0\,(cm^{-3}s^{-1})$, considering linearly anisotropic scattering [13]. Fig. 2 (not drawn to scale), presents a quarter of this configuration with the boundary conditions used to perform the simulation.

Table 1 lists the values of the material parameters in each material zone. The objective in this experiment is to determine the neutron leakage through the upper( $\widehat{J}_+(x)$ ) and right( $\widetilde{J}_+(y)$ ) boundaries of the domain represented in Fig. 2. These leakage values are calculated using the Eqs. 26 and 27

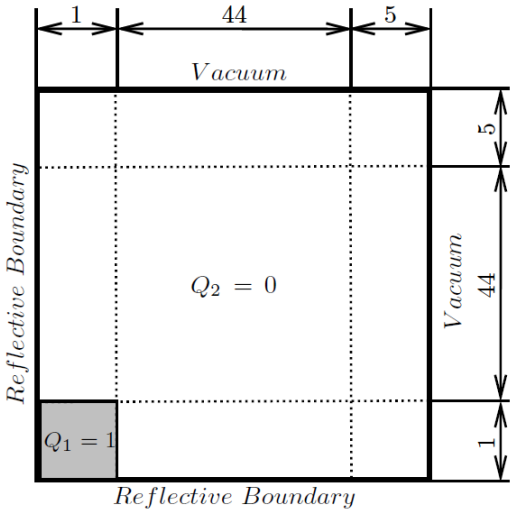



Figure 2: First Model problem configuration.

Table 1: Material parameters

| Material Zone | $\sigma_T(cm^{-1})$ | $\sigma_S^{(0)}(cm^{-1})$ | $\sigma_S^{(1)}(cm^{-1})$ |
|---|---|---|---|
| 1 | 0.80 | 0.40 | 0.20 |
| 2 | 1.00 | 0.95 | 0.50 |

$$\widetilde{J}_+(51) = \frac{1}{4}\sum_{j=1}^{J}\sum_{\mathrm{g}=1}^{2}\sum_{\mu_n>0}\mu_n\widetilde{\psi}_{n,g,j}(51)h_{y_j}\omega_n\,, \tag{26}$$

$$\widehat{J}_+(51) = \frac{1}{4}\sum_{i=1}^{I}\sum_{\mathrm{g}=1}^{2}\sum_{\eta_n>0}\eta_n\widehat{\psi}_{n,g,i}(51)h_{x_i}\omega_n\,, \tag{27}$$

The stopping criterion requires that the relative deviation between two consecutive estimates for the scalar flux on the faces of the domain nodes to be less than or equal to $10^{-7}$.

The Table 2 is shown the numerical results of the right and upper boundary leakage calculations besides the relative deviations $\delta_U(\%)$ and $(\delta_R(\%))$ for the $SGF-CN$ and $SDM-CN$, using as reference the value obtained with the $DD$ method using a $20\times 880\times 100$ nodes per region in the $x$ and $y$ direction, when it reaches the fine mesh size, which is the size that for the scalar fluxes in the sixth decimal place do not have a significant variation. To calculate the relative deviations $\delta(\%)$, in both cases, we use the expression

$$\delta(\%) = \left|\frac{S_{DD}-S_m}{S_{DD}}\right|\times 100, \tag{28}$$

where $S_{DD}$ is the neutron leakage value obtained with the $DD$ method used as a reference and $S_m$ represents the neutron leakage value generated by each of the methods used to calculate such leakage in the specified boundaries.

As can be seen, in Table 2 the results obtained for the leaks in both boundaries are symmetrical and as the spatial grid becomes thinner, the results generated by both coarse mesh methods converge to the same result. The values for the relative percentage deviations of the methods $SGF-CN$ and $SDM-CN$ when comparing them with the $DD$ method, present values less than 3 %.

The second model problem is a fixed source experiment in absorbing medium, which was suggested by the Argonne Code Center Benchmark Problems Committee and models a realistic shielding situation [8]. This problem has been designed to provide stringent tests for two-dimensional geometry transport codes with two energy groups [23].

Table 2: Neutrons leakage for Model Problem 1

| $\Omega_x \times \Omega_y$ spatial grid | Method | Upper boundary leakage ( $\widehat{J}_+(51)$ ) | $\delta_U(\%)^b$ | Right boundary leakage ( $\widetilde{J}_+(51)$ ) | $\delta_R(\%)$ |
|---|---|---|---|---|---|
| 20×880×100 | DD | 4.99400E-06[c] | – | 4.99400E-06 | – |
| 1×17×2 | SGF-CN | 4.88894E-06 | 2.1039 | 4.88894E-06 | 2.1039 |
| | SDM-CN | 5.13538E-06 | 2.8310 | 5.13538E-06 | 2.8310 |
| 1×26×3 | SGF-CN | 4.94060E-06 | 1.0693 | 4.94060E-06 | 1.0693 |
| | SDM-CN | 5.05927E-06 | 1.3070 | 5.05927E-06 | 1.3070 |
| 1×44×5 | SGF-CN | 4.97479E-06 | 0.3847 | 4.97479E-06 | 0.3847 |
| | SDM-CN | 4.97479E-06 | 0.3847 | 4.97479E-06 | 0.3847 |
| 2×88×10 | SGF-CN | 4.98905E-06 | 0.0991 | 4.98905E-06 | 0.0991 |
| | SDM-CN | 4.98905E-06 | 0.0991 | 4.98905E-06 | 0.0991 |

[a] Neutrons leakage : $\text{cm}^{-2}\ \text{s}^{-1}$.
[b] Relative deviations.
[c] Read: $4.99400 \times 10^{-6}$ .

The problem geometry is illustrated in Fig. 3. The macroscopic cross sections for the homogeneous material of the system and the source density are listed in Table 3.

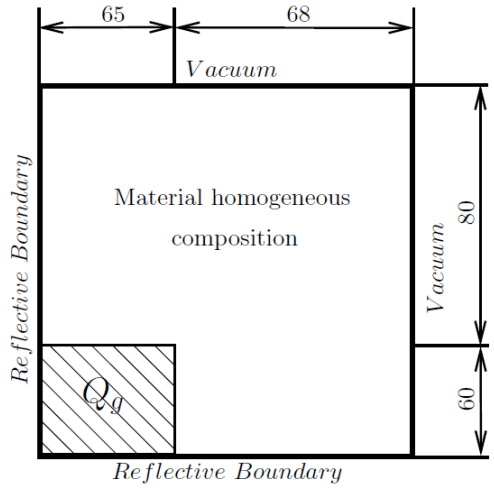



Figure 3: Second model problem configuration.

To simulate this problem using the *SDM-CN* method, a spatial discretization grid it is defined as follows, in the direction of $x$, where it is the region with the uniform spatial source ($0 \leq x \leq 65$) was divided into 13 nodes and the region without source ($65 \leq x \leq 133$) into 14 nodes. Similarly, in the direction of the spatial variable $y$, it was divided into 12 nodes in the region with source ($0 \leq x \leq 60$) and 16 nodes in the region without source ($60 \leq x \leq 140$).

To compare the results obtained by the *SDM-CN* method, we use the reported results for this problem by Dias in [23], using the *DOT-II* and *TWOTRAN* codes together to the results of the *SGF-CN* method reported by Menezes [23]. The Table 4 shows the numerical results obtained for the total leakage for both energy groups, $J_+^{T_g}$, at the right boundary of the system shown in Fig. 3. The results listed in [23] for code *TWOTRAN* considering a spatial discretization grid of 6804 nodes, $(39 \times 42) \times (36 \times 48)$, were used as reference for calculating the relative relative deviation of all methods addressed in this experiment using a spatial discretization grid of 756 nodes, $(13 \times 14) \times (12 \times 16)$. Were considered $S_8$ and $S_{12}$ sets of the Level Symmetric Quadrature, $\text{LQ}_N$.

As can be seen in Table 4, the relative percentage deviations of the results generated by the *SDM-CN* method for the right boundary leakage were always smaller than the relative deviations generated by the *DOT–II* and *TWOTRAN* similar to the behavior of the *SGF–CN* method. It may also be noted that the relative percent deviations of the method results in the SDM-CN method decreased with increasing quadrature of the symmetry level.

Table 3: Macroscopic Cross Sections ($cm^{-1}$) and source density ($neutrons/cm^3$) for the second model problem

| | $g=1$ | $g=2$ |
|---|---|---|
| $\sigma_{T_g}$ | 0.092104 | 0.100877 |
| $Q_g$ | 0.006546 | 0.017701 |
| | $\sigma^{(0)}_{s_{g'\to g}}(cm^{-1})$ | |
| $g'=1$ | 0.006947 | 0.023434 |
| $g'=2$ | 0.000000 | 0.004850 |

Table 4: Neutron leakage [a] by right boundary

| $J^{T_g}_+$ | | | | | | |
|---|---|---|---|---|---|---|
| $S_N$ | g | Fine mesh reference | $TWOTRAN$ | $DOT-II$ | $SGF-CN$ | $SDM-CN$ |
| 8 | 1 | 5.7400E-04[b] | 5.0000E-04 (12.8920 %)[c] | 4.9900E-04 (13.0662 %) | 5.4744E-04 (4.6272 %) | 5.4744E-04 (4.6279 %) |
| | 2 | 9.2100E-04 | 8.0000E-04 (13.1379 %) | 7.7500E-04 (15.8523 %) | 8.7832E-04 (4.6341 %) | 8.7832E-04 (4.6346 %) |
| 12 | 1 | 5.5700E-04 | 4.9600E-04 (10.9515 %) | 4.9900E-04 (10.4129 %) | 5.4833E-04 (1.5566 %) | 5.5360E-04 (0.6110 %) |
| | 2 | 8.9100E-04 | 7.7600E-04 (12.9068 %) | 7.7500E-04 (13.0191 %) | 8.7868E-04 (1.3827 %) | 8.9028E-04 (0.0806 %) |

[a] Neutrons leakage : $cm^{-2}\ s^{-1}$,
[b] Read: 5.7400 x $10^{-4}$,
[c] Percent relative deviation .

# 5 Discussion

In this paper, a two-dimensional coarse-mesh numerical method, for multigroup fixed source linearly anisotropic $S_N$ problem in $X, Y$ geometry, $SDM-CN$, has been described and developed. The multigroup $SDM-CN$ discretization scheme preserves the general solution of the multigroup $S_N$ equation in each spatial node, converges to numerical results that are continuous across each node interface and satisfies the external boundary conditions whether the mesh size order or quadrature set used. The $SDM-CN$ method converges to approximate numerical solutions that coincide with the numerical results obtained from the solution of the analyzed $S_N$ problem regardless the definition of the spatial grid or the angular quadrature used, same as the $SGF-CN$ method while the fine-mesh DD method, *DOT–II* and *TWOTRAN* solution are not. When calculating the transverse leakage terms, in the method *SDM–CN*, these are approximated by constants. These relative deviations can be attenuated if a better approximation is made for the transverse leakage terms.

Our expectation for the future of this methodology is that, due to its simplicity of implementation, the $SDM-$ $-CN$ method will give us CPU times, for the modelings executed, lower than the *DD* method and other methods used for the neutron transport calculations.

For future works, we plan to implement different and more complex model problems, reporting on the numerical method results after they have been executed and thoroughly tested.

# References

[1] J. M. Hammersley and D. C. Handscomb, *Monte Carlo Methods.* London, UK: Methuen & Co, 1964.

[2] E. E. Lewis and W. F. Miller, *Computational methods of neutron transport*. Illinois, USA: American Nuclear Society, 1993.

[3] J. J. Duderstadt and W. R. Martin, *Transport Theory*. New York, USA: Wiley–Interscience, 1979.

[4] A. A. Mohamad, "Local analytical discrete ordinate method for the solution of the radiative transfer equation," *International Journal of Heat and Mass Transfer*, vol. 39, no. 9, pp. 1859–1864, 1996. Available at: https://doi.org/10.1016/0017-9310(95)00282-0

[5] C. E. Siewert, "The $F_N$ method for solving radiative transfer problems in plane geometry," *Astrophysics and Space Science*, vol. 58, no. 2, pp. 131–137, 1978. Available at: https://doi.org/10.1007/BF00645380

[6] A. Badruzzaman, *Nodal methods in transport theory.* New York, USA: Plenum Press, 1990, vol. 21, ch. 3.

[7] R. D. Laurence, "Progress in nodal methods for the neutron diffusion and transport equations," *Progress in Nuclear Energy*, vol. 17, pp. 271–301, 1986. Available at: https://doi.org/10.1016/0149-1970(86)90034-X

[8] W. A. Menezes, "Métodos espectronodais para cálculos de partículas neutras com fonte fixa na formulação de ordenadas discretas e multigrupo de energia." Ph.D. dissertation, Programa de Pós-Graduação em Modelagem Computacional, Universidade do Estado do Rio de Janeiro, Nova Friburgo, Brasil, 2012. Available at: http://www.bdtd.uerj.br/handle/1/13651

[9] A. M. Oliva, "Método espectral determinístico para a solução de problemas de transporte de nêutrons usando a formulação das ordenadas discretas," Ph.D. dissertation, Programa de Pós-Graduação em Modelagem Computacional, Universidade do Estado do Rio de Janeiro, Nova Friburgo, Brasil, 2018. Available at: https://www.bdtd.uerj.br:8443/bitstream/1/13719/1/Tese_AmauryMunozOliva.pdf

[10] O. Da Silva, "Um método de matriz resposta para cálculos de transporte multigrupos de energia na formulação de ordenadas discretas em meios não-multiplicativos," Ph.D. dissertation, Programa de Pós-Graduação em Modelagem Computacional, Universidade do Estado do Rio de Janeiro., Nova Friburgo, Brasil, 2018. Available at: http://www.bdtd.uerj.br/handle/1/13715

[11] R. Barros and E. Larsen, "A numerical method for one-group slab-geometry discrete ordinates problems with no spatial truncation error," *Nuclear Science and Engineering*, vol. 104, no. 3, pp. 199–208, 1990. Available at: https://doi.org/10.13182/NSE90-A23719

[12] R. C. Barros, "A spectral nodal method for the solution of discrete ordinates problems in one and two dimensional cartesian geometry." Ph.D. dissertation, The University of Michigan, Ann Arbor, Michigan, United States., 1990. Available at: https://deepblue.lib.umich.edu/handle/2027.42/105093

[13] R. C. Barros and E. W. Larsen, "A spectral nodal method for one-group $X,Y$-geometry discrete ordinates problems," *Nuclear Science and Engineering*, vol. 111, no. 1, pp. 34–45, 1992. Available at: https://doi.org/10.13182/NSE92-A23921

[14] R. Barros and E. Larsen, "A numerical method for multigroup slab-geometry discrete ordinates problems with no spatial truncation error," *Transport Theory and Statistical Physics*, vol. 20, no. 5-6, pp. 441–462, 1991. Available at: https://doi.org/10.1080/00411459108203914

[15] E. W. Larsen, "Spectral analysis of numerical methods for discrete-ordinates problems. i," *Transp. Theory Stat. Phys.; (United States)*, vol. 15:1, 1 1986. Available at: https://www.osti.gov/biblio/5871918

[16] A. Oliva, H. Alves Filho, D. J. Silva, and C. R. García, "Computer Deterministic Modelling of Nuclear Problems using Nodal Methods," in *Proceeding Series of the Brazilian Society of Computational and Applied Mathematicsl–CNMAC 2016*, ser. ISSN: 2359–0793. Gramado, RS, Brazil: Sociedade de Matemática Aplicada e Computacional(SBMAC), 2016.

[17] ——, "Spectral nodal methodology for multigroup slab-geometry discrete ordinates neutron transport problems with linearly anisotropic scattering," in *International Nuclear Atlantic Conference–INAC 2017*, ser. ISBN: 978–85–99141–07–6. Belo Horizonte, MG, Brazil: Associação Brasileira de Energia Nuclear (ABEN), 2017.

[18] ——, "The spectral nodal method applied to multigroup $S_N$ neutron transport problems in one–dimensional geometry with fixed–source," *Progress in Nuclear Energy*, vol. 105, pp. 106–113, 2018. Available at: https://doi.org/10.1016/j.pnucene.2017.12.017

[19] K. M. Case and P. F. Zweifel, *Linear transport theory.*, ser. Addison-Wesley series in nuclear engineering. USA: Reading, Mass., Addison-Wesley Pub. Co, 1967.

[20] W. Menezes, H. A. Filho, and R. Barros, "Spectral green's function nodal method for multigroup $s_n$ problems with anisotropic scattering in slab-geometry non-multiplying media," *Annals of Nuclear Energy*, vol. 64, pp. 270–275, 2014. Available at: https://doi.org/10.1016/j.anucene.2013.09.023

[21] A. M. Oliva, H. Alves Filho, D. J. SILVA, and C. R. García, "The spectral nodal method applied to multigroup $S_N$ neutron transport problems in one–dimensional geometry with fixed–source," *Progress in Nuclear Energy*, vol. 105, pp. 106–113, 2018.

[22] A. Oliva, H. Alves Filho, R. C. Barros, and J. Pérez Curbelo, "The Spectral Deterministic Method applied to neutron fixed-source discrete ordinates problems in X, Y-geometry for multigroup calculations," in *International Nuclear Atlantic Conference–INAC 2019*, ser. ISBN: 978–85–99141–08–3. Santos, SP, Brazil: Associação Brasileira de Energia Nuclear (ABEN), 2019.

[23] A. F. Dias, "Estudo e aplicação dos códigos ANISN e DOT-II em problemas de física de reatores," Master's thesis, Instituto de Pesquisas Energéticas e Nucleares - IPEN/CNEN-SP, SP, Brasil, 1980. Available at: http://repositorio.ipen.br/handle/123456789/9642